2.4/5.7-GHz Dual-Band Dual-Conversion Architecture With Correlated *LO* Signal Generators

Jin-Siang Syu[1], Chinchun Meng[1], Sheng-Wen Yu[1], Tzung-Han Wu[1] and Guo-Wei Huang[2, 3]

[1]Department of Communication Engineering, National Chiao Tung University, Hsinchu, 300 Taiwan, R.O.C.

[2]Department of Electronics Engineering, National Chiao Tung University, Hsinchu, 300 Taiwan, R.O.C.

[3]National Nano Device Laboratories, Hsinchu, 300 Taiwan, R.O.C.

***Abstract* — A 2.4/5.7-GHz dual-band dual-conversion downconverter is demonstrated using 0.35-μm SiGe hetero-junction bipolar transistor (HBT) technology. This downconverter employs a complex dual-conversion system and a complex filter to reject the first and second image signals, respectively. The LO_1 frequency is 2.5 times the LO_2 frequency and is generated by a divide-by-two divider, a frequency doubler and a single-sideband up-converter. As a result, the correlated *LO* signals maintain excellent image-rejection performance of the dual-conversion system while only one *LO* input is needed. The downconverter achieves a 40/39-dB image-rejection ratio of the first image and a 44/46-dB image-rejection ratio of the second image for 2.4/5.7-GHz modes, respectively.**

***Index Terms* —Wireless LAN, dual-band, SiGe heterojunction bipolar transistor (HBT), low-*IF*, image rejection.**

I. Introduction

Compared with two (or multiple)-separate-system solutions for multi-band applications, the dual-band (or multi-band) reconfigurable system has a relatively high integration level. For dual-band transceivers, the direct-conversion architectures were demonstrated [1]-[4]. Besides, some dual-band dual-conversion systems were demonstrated while the signal was down-converted to baseband (IF_2=0) at the second stage; thus, there is no second image problem [5] but the flicker noise and dc offset problems arise and need more efforts to solve [6]-[7]. Most of these zero-*IF* multi-band receivers require more than one local oscillator [1]-[3]. Since IF_2=0, it is difficult to use one VCO covering both bands. The extra VCO may cause substrate cross-talk and spurious signals.

In this paper, a 2.4/5.7-GHz dual-band low-*IF* system for WLAN 802.11 a/g applications is demonstrated. Since the low-*IF* architecture keeps the *IF* frequency flexible, the LO_1 and LO_2 can be set as a fractional multiple of each other. Thus, the LO_1 frequency is 2.5 times the LO_2 frequency in this work and thus only one *LO* signal source is needed. Besides, correlated *LO* signals can maintain an excellent image-rejection performance as long as phase errors at the first and second *LO* differential-quadrature signals are the same [8].

The dual-conversion low-*IF* system of this work combines the Weaver architecture [8]-[10] and Hartley architecture [11]. The former is a complex dual-conversion topology that removes the image signal by a frequency-shifting mechanism while the latter is a complex down-conversion with a complex poly-phase filter to remove the image. In a complex mixer topology, the signal spectrum shifts in one way, either upwards or downwards, as long as the *LO* signal is perfectly quadrature [9]. As a result, different polarities of the *LO* signal result in different operating modes.

The demonstrated dual-band system performs excellent image-rejection performance because the double-quadrature system of the second stage has much immunity of an amplitude/phase error not only from a signal imbalance but also from device mismatches in the mixers.

II. Circuit Design

The block diagram of the 2.4/5.7-GHz dual-band dual-conversion downconverter is shown in Fig. 1. This circuitry consists of a single-quadrature system (two mixers) at the first stage, a double-quadrature system (four mixers) at the following stage and an *LO* generator generating differential-quadrature signals of LO_1 and LO_2. An active Gilbert mixer is employed in both the first- and second-stage mixers for its advantages of a higher gain and a lower *LO* power requirement. Besides, the first-stage mixer is a micromixer topology [12] consisting of common-emitter and common-base configurations at the input stage; thus, the balanced output and wideband matching can be easily achieved.

The frequency multiplier with a multiple of 2.5 consists of a frequency doubler (×2) and a frequency divider (÷2). After the mixing operation of a single-sideband (SSB) up-converter, the LO_1 ($2.5\times LO_2$) signal is thus generated. Both differential-quadrature signals of the LO_1 and LO_2 are generated by a two-section poly-phase filter with the center frequency of 4.05 and 1.62 GHz, respectively. Figure 2(a) shows the block diagram of the static divider consisting of two D-latches realized by emitter-coupled logic. The schematic of the D-latch, consisting of the sample and hold stages, is shown in Fig. 2(b). Instead of using a simple cross-coupled pair, the common-collector configuration is inserted into the positive feedback loop at the hold stage to achieve a wider output swing and a higher achievable operating frequency.

Figure 3(a) shows the function block of the multiplier while the schematic of the multiplier is shown in Fig. 3(b). If $f_1 \neq f_2$, the multiplier is an SSB up-converter while the (f_1-f_2) frequency component is cancelled if the two input signals have a perfect quadrature phase. On the other hand, if $f_1=f_2=f_0$,

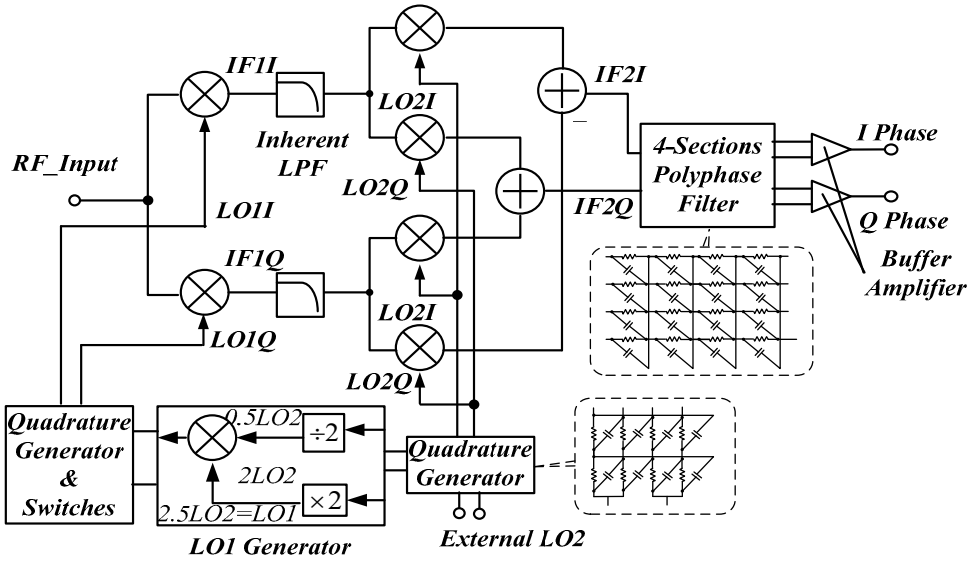

Fig. 1. Block diagram of the 2.4/5.7-GHz dual-band dual-conversion downconverter with correlated LO signal generators.

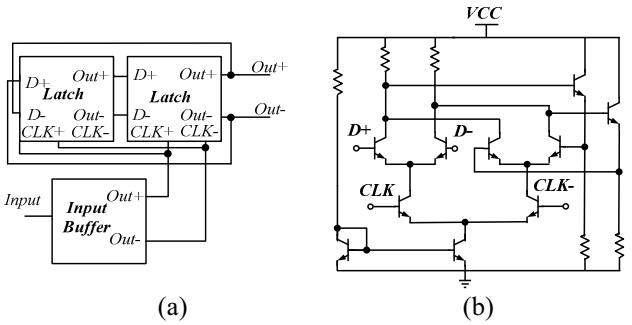

(a) (b)

Fig. 2. (a) Block diagram of the static divide-by-two divider (2) the D-latch cell used in the divider.

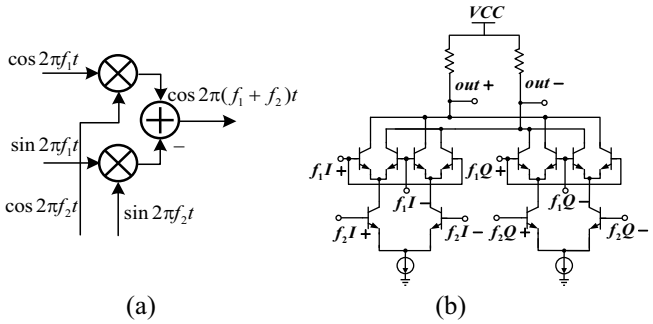

(a) (b)

Fig. 3. (a) Function block of the multiplier which can be utilized as a single-sideband upconverter and a frequency doubler (b) schematic of the multiplier.

the circuit becomes a frequency doubler with the output frequency of $2f_0$.

In the complex mixer topology of the first stage, the mixing operation leads to the frequency spectrum right-shifting, i.e., $f_{IF1}=(-f_{RF})+f_{LO1}$, if the differential-quadrature LO_1 has the positive output sequence (0º, 90º, 180º and 270º). On the other hand, if the polarity of the LO_1 is reversed, the output

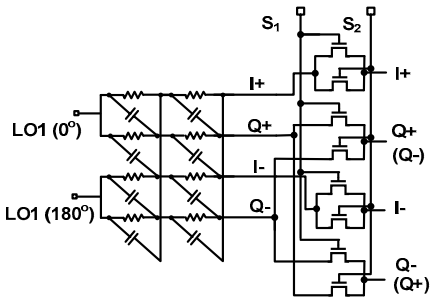

Fig. 4. Function block of the multiplier which can be utilized as a single-sideband upconverter and a frequency doubler (b) schematic of the multiplier.

spectrum is left-shifting, i.e., $f_{IF}=f_{RF}-f_{LO1}$. By setting the LO_1 frequency at 4.05 GHz, halfway between 2.4 GHz and 5.7 GHz, the 2.4-GHz receiving mode employs a positive LO_1 sequence (0º, 90º, 180º and 270º) while the 5.7-GHz receiving mode employs a negative LO_1 sequence (0º, 270º, 180º and 90º). As a result, the outputs at the first stage are both down-converted to 1.65 GHz with positive *I/Q* output sequence when the desired signal is received for both modes. Therefore, the dual-band operation can be achieved. The schematic of the switch of the *I/Q* signal polarity is shown in Fig. 4. When $(S_1,S_2)=(L,H)$, the 5.7-GHz band is selected. On the other hand, the 2.4-GHz band is chosen if $(S_1,S_2)=(H,L)$.

III. Measurement Results

Figure 5 shows the microphoto of the 2.4/5.7-GHz dual-band dual-conversion downconverter with correlated *LO* signal generators and the die size is 1.63x1.52 mm^2. On-wafer measurement is employed for the *RF* performance. The total power consumption is 198 mW at a 3.3-V supply. Figure 6 shows the conversion gain (CG) and the single-sideband noise

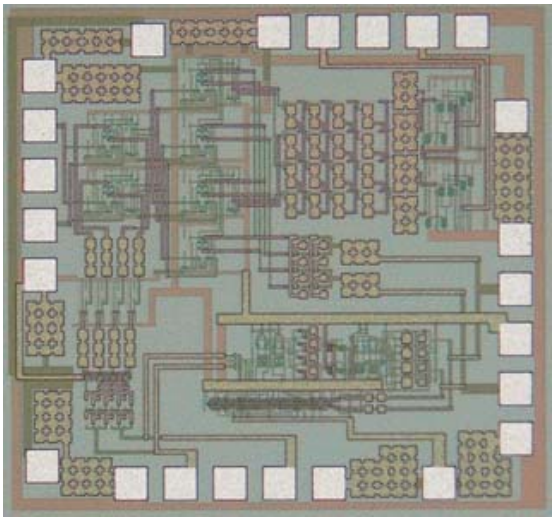

Fig. 5. The microphoto of the 2.4/5.7-GHz dual-band dual-conversion downconverter with correlated LO signal generators.

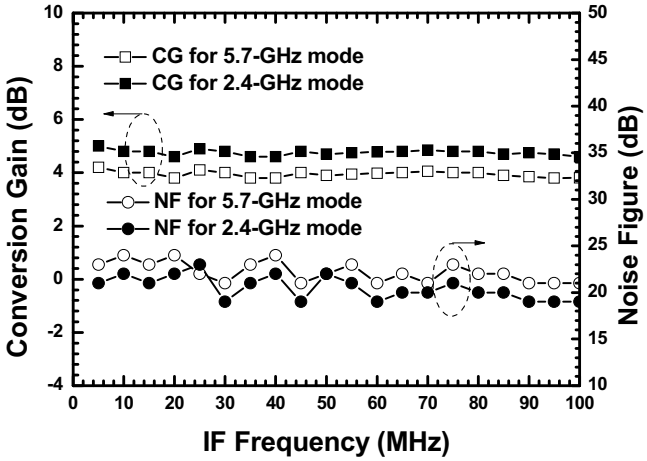

Fig. 6. Conversion gain and noise figure of the 2.4/5.7-GHz dual-band dual-conversion downconverter with correlated LO signal generators.

figure (SSB-NF) of 2.4/5.7-GHz bands The CG is 5/4 dB while the NF is about 20 dB for 2.4/5.7-GHz band while the *IF* frequency is below 100 MHz and the *LO* power is only 2 dBm. Besides, the image-rejection ratios (*IRR*s) of both the first and second image signals for 2.4-GHz band are shown in Fig. 7. The IRR_1 is above 40 dB and is flat due to the one-way frequency shifting. Compared with the IRR_1, the IRR_2 is 44-dB within a narrow band from 15 to 45 MHz due to the frequency response of the four-section poly-phase filter following the second-stage mixers. On the other hand, the IRR_1 and IRR_2 are 39 and 46 dB within the *IF* bands from 15 to 45 MHz for the 5.7-GHz mode as shown in Fig 8. Figure 9 shows the power performance of both 2.4/5.7-GHz bands. The IP_{1dB} is -12/-9 dBm while the IIP_3 is 2/6 dBm for 2.4/5.7-GHz band when *IF*=30 MHz. The output waveform of both *I/Q* channels are shown in Fig. 10 and the figure shows a 0.46 dB magnitude mismatch and a 0.62° phase error.

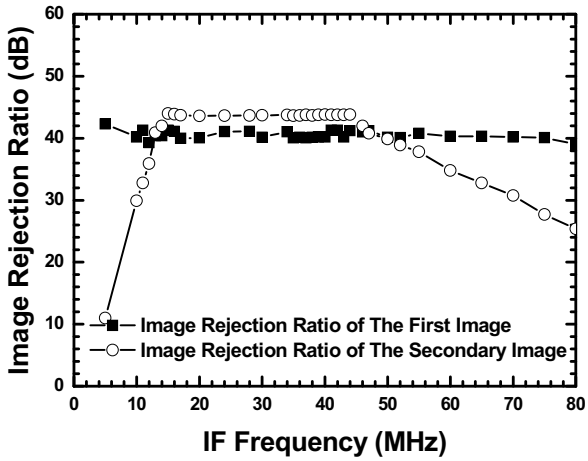

Fig. 7. Image rejection ratios of the first and second image signals at 2.4-GHz mode of the dual-band dual-conversion downconverter.

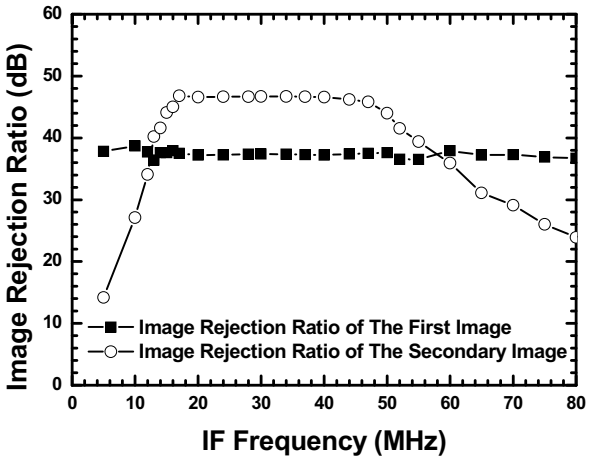

Fig. 8. Image rejection ratios of the first and second image signals at 5.7-GHz mode of the dual-band dual-conversion downconverter .

IV. Conclusion

A highly-merged dual-band dual-conversion low-*IF* downconverter for WLAN 802.11 a/g applications is demonstrated in this paper. The band selection is achieved by changing the polarity of the first *LO* signals and thus 2.4-GHz and 5.7-GHz bands are the image band of each other. Besides, only one signal generator is needed for the dual-conversion system. Since the two *LO* signals are highly correlated, excellent *IRR*s still maintain. As a result, IRR_1/IRR_2 for 2.4-GHz mode are 40/44 dB while a 39-dB IRR_1 and a 46-dB IRR_2 are achieved for the 5.7-GHz mode when *IF* frequency ranging from 15 to 45 MHz.

Acknowledgement

This work is supported by National Science Council of Taiwan, Republic of China under contract numbers NSC 95-2221-E-009-043-MY3, NSC 97-2221-E-009-171 and NSC 98-

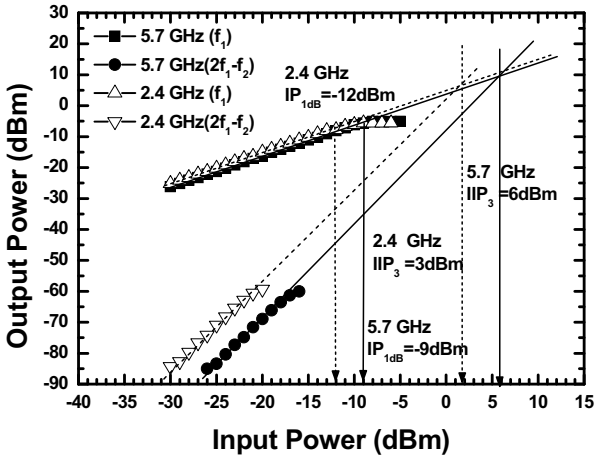

Fig. 9. Power performance of the 2.4/5.7-GHz dual-band dual-conversion downconverter with correlated LO signal generators.

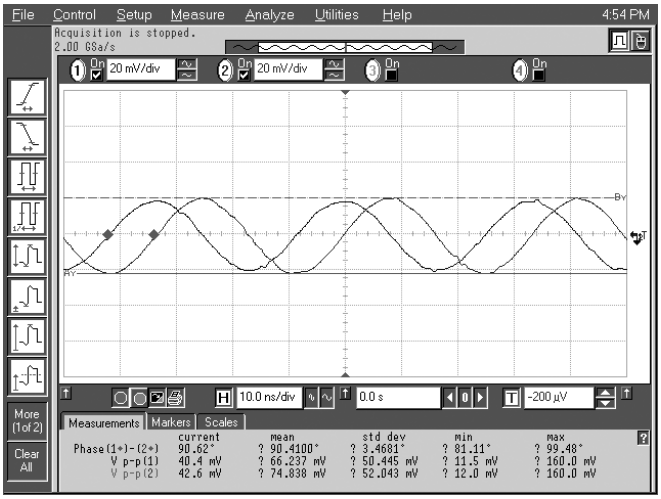

Fig. 10. Output I/Q waveforms of the 2.4/5.7-GHz dual-band dual-conversion downconverter with correlated LO signal generators.

2218-E-009-008-MY3, by the Ministry of Economic Affairs of Taiwan under contract number 96-EC-17-A-05-S1-020, and by MoE ATU Program under contract number 95W803. The authors would like to thank National Chip Implementation Center (CIC) for technical support.

REFERENCES

[1] R. Ahola, A. Aktas, J. Wilson, K. R. Rao, F. Jonsson, I. Hyyryläinen, A. Brolin, T. Hakala, A. Friman, T. Mäkiniemi, J. Hanze, M. Sandén, D. Wallner, Y. Guo, T. Lagerstam, L. Noguer, T. Knuuttila, P. Olofsson, and M. Ismail, "A single-chip CMOS transceiver for 802.11a/b/g wireless LANs," *IEEE J. Solid-State Circuits*, vol. 39, no. 12, pp.2250-2258, Dec. 2004.

[2] O. Charlon, M. Locher, H. A. Visser, D. Duperray, J. Chen, M. Judson, A. L. Landesman, C. Hritz, U. Kohlschuetter, Y. Zhang, C. Ramesh, A. Daanen, M. Gao, S. Haas, V. Maheshwari, A. Bury, G. Nitsche, A. Wrzyszcz, W. R. White, H. Bonakdar, R. E. Waffaoui, and M. Bracey, "A low-power high-performance SiGe BiCMOS 802.11 a/b/g transceiver IC for cellular and Bluetooth co-existence applications", *IEEE J. Solid-State Circuits*, vol. 41, no. 7, pp. 1503-1512, Jul. 2006.

[3] M. Zargari, M. Terrovitis, S. H. M. Jen, B. J. Kaczynski, M. Lee, M. P. Mack, S. S. Mehta, S. Mendis, K. Onodera, H. Samavati, W. W. Si, K. Singh, A. Tabatabaei, D. Weber, D. K. Su, and B. A. Wooley, "A single-chip dual-band tri-mode CMOS transceiver for IEEE 802.11a/b/g wireless LAN", *IEEE J. Solid-State Circuits*, vol. 39, no. 12, pp. 2239-2249, Dec. 2004.

[4] A. Behzad, K. A. Carter, H. –M. Chien, S. Wu, M.-A. Pan, C. P. Lee, Q. Li, J. C. Leete, S. Au, M. S. Kappes, Z. Zhou, D. Ojo, L. Zhang, A. Zolfaghari, J. Castanada, H. Darabi, B. Yeung, A. Rofougaran, M. Rofougaran, J. Trachewsky, T. Moorti, R. Gaikwad, A. Bagchi, J. S. Hammerschmidt, J. Pattin, J. J. Rael, and B. Marholev, "A fully integrated MIMO multiband direct conversion CMOS transceiver for WLAN applications (802.11n)", *IEEE J. Solid-State Circuits*, vol. 42, no. 12, pp. 2795-2808, Dec. 2007.

[5] S. Wu and B. Razavi, "A 900-MHz/1.8-GHz CMOS receiver for dual-band applications," *IEEE J. Solid-State Circuits*, vol. 33, no.12, pp. 2178–2185, Dec. 1998.

[6] A. A. Abidi, "Direct-conversion radio transceivers for digital communications," *IEEE J. Solid-State Circuits*, vol. 30, no. 12, pp.1399-1410, Dec. 1995.

[7] H. Darabi, and A. A. Abidi, "Noise in RF-CMOS mixers: a simple physical model," *IEEE J. Solid-State Circuits*, vol. 35, no. 1, pp. 15-25, Jan. 2000.

[8] T. H. Wu, and C. C. Meng, "5.2/5.7GHz 48dB Image Rejection GaInP/GaAs HBT Weaver Down-Converter Using LO Frequency Quadrupler," *IEEE J. Solid-State Circuits,* vol. 41, no. 11, pp.2468-2480, Nov. 2006.

[9] D. Weaver, "A third method of generation and detection of single-sideband signals," *Proceedings of The IRE*, pp. 1703-1705, Dec. 1956.

[10] J. C. Rudell, J.-J. Ou, T. B. Cho, G. Chien, F. Brianti, J. A. Weldon, and P. R. Gray, "A 1.9-GHz wide-band IF double conversion CMOS integrated receiver for cordless telephone applications," *IEEE J. Solid-State Circuits*, vol. 32, no.12, pp. 2071-1088, Dec. 1997.

[11] F. Behbahani, Y. Kishigami, J. Leete, and A. A. Abidi, "CMOS mixers and polyphase filters for large image rejection," *IEEE J. Solid-State Circuits*, vol. 36, no.6, pp. 873-887, Jun. 2001.

[12] B. Gilbert, "The MICROMIXER: A highly linear variant of the Gilbert mixer using a bisymmetric Class-AB input stage," *IEEE J. Solid-State Circuits*, vol. 32, pp. 1412-1423, Sept. 1997.